

Lawin Transformer: Improving New-Era Vision Backbones with Multi-Scale Representations for Semantic Segmentation

Haotian Yan, Chuang Zhang, Ming Wu
 Pris Lab, Beijing University of Posts and Telecommunications
 {yanhaotian, zhangchuang, wuming}@bupt.edu.cn

Abstract

The multi-level aggregation (MLA) module has emerged as a critical component for advancing new-era vision backbones in semantic segmentation. In this paper, we propose Lawin (large window) Transformer, a novel MLA architecture that creatively utilizes multi-scale feature maps from the vision backbone. At the core of Lawin Transformer is the Lawin attention, a newly designed window attention mechanism capable of querying much larger context windows than local windows. We focus on studying the efficient and simplistic application of the large-window paradigm, allowing for flexible regulation of the ratio of large context to query and capturing multi-scale representations. We validate the effectiveness of Lawin Transformer on Cityscapes and ADE20K, consistently demonstrating great superiority to widely-used MLA modules when combined with new-era vision backbones. The code is available at <https://github.com/yan-hao-tian/lawin>.

1. Introduction

The new-era backbone is referred to as the Vision Transformer [5, 7, 10] and ConvNets with new-era model designs [6, 8] mostly derived from Vision Transformers. When utilizing them in semantic segmentation, the multi-layer aggregation (MLA) module, an expert at aggregating multi-scale feature maps of backbone, gains more and more popularity. UperNet [9], in particular, has contributed much to the advancement of semantic segmentation in the new era [7, 8]. Despite a powerful MLA module, UperNet is somewhat computationally expensive. Hence, some papers propose alternative solutions to improve efficiency. For instance, SegFormer [10] designs a very simple but effective MLP-decoder, while MaskFormer [3] applies a straightforward feature pyramid network (FPN) as the pixel decoder for semantic mask classification.

This paper aims to design a new MLA module in order to balance performance and efficiency for new-era vision

backbones in semantic segmentation. By revisiting previous works, we propose Lawin Transformer incorporating four key ideas.

- 1) The essence of MLA lies in the capability of employing multi-scale representations. The way of generating and leveraging strong representations is prominent and should be computationally efficient. We propose the Lawin attention adept at this in a relational manner.
- 2) The spatial conv layer has higher computation costs than the linear layer. The separable conv has lower computation costs but wastes more memory and latency. Lawin Transformer consists of just linear layers and a few conv layers at the same cost as linear layers.
- 3) Feature maps from the backbone constitute a feature pyramid. The feature map with larger spatial sizes has more spatial information, and the smaller one has strong representations. Thus, all levels of the pyramid are irreplaceable and should be effectively exploited.
- 4) From 3), performing more operations on the large feature map brings both increased computation costs and performance gains. A good trade-off between performance and efficiency requires a computation-friendly assignment of operations on multi-level feature maps.

2. Approach

2.1. Lawin Attention

The central function of MLA is exploiting multi-scale feature maps of the backbone so we first introduce the large-window paradigm and the application thereof on capturing multi-scale representations.

Local window attention enjoys a reputation for window-limited computation and memory. The computation cost can be formulated as:

$$\Omega(\text{WA}) = 4(HW)C^2 + 2(HW)P^2C, \quad (1)$$

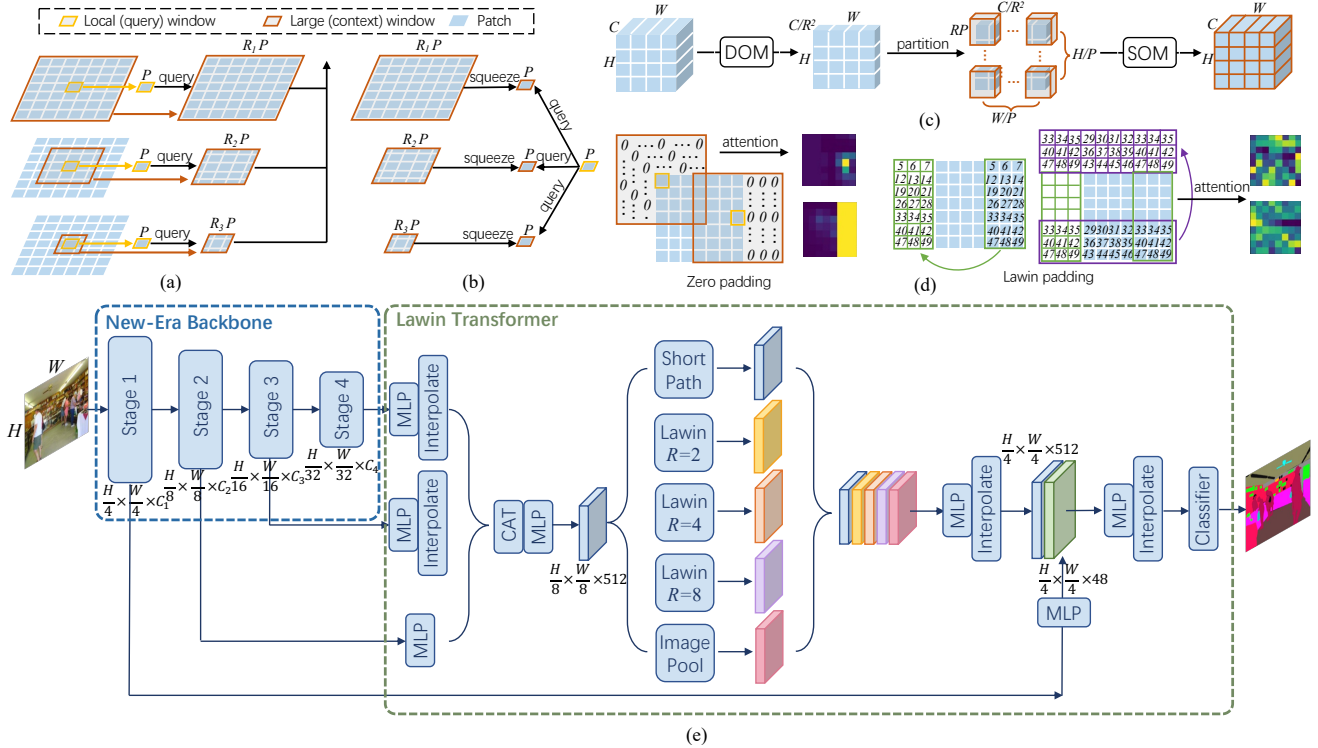


Figure 1. (a) Applying the large-window paradigm to capture multi-scale representations. (b) Simply squeezing the large context patch to maintain the local window computation. (c) DOM layer and SOM layer. (d) Lawin padding mode versus zero padding mode. (e) Illustration of the overall structure of Lawin Transformer. “MLP” denotes one linear layer. “CAT” denotes concatenating features.

where H , W , and C denote the height, width, and channel number of the input, and P denotes the patch size of the local window. Notably, the first term is on linear mappings, *i.e.* q , k , v , and out , and the second term is on the attention computation that is acted on the local window. The memory cost of attention matrices is $(HW)P^2$ accordingly.

Different from global self-attention, the receptive field of the pixel in window attention is the local window where it is located. Through decoupling the query and context in window attention and regulating the size ratio of the context window to the query window, a new multi-scale paradigm similar to atrous convolutions with multiple atrous rates can be attained, as visualized in Fig. 1. a. Although an intuitive methodology, the large-window paradigm incurs considerable computation and memory costs. Denoting the ratio as R , we list the computation cost:

$$\Omega(\text{WA}) = 2(R^2 + 1)(HW)C^2 + 2(HW)(RP)^2C. \quad (2)$$

Besides, the memory cost is unaffordable. The memory for the large context, k , and v , is R^2 times than the local counterpart (R^2HWC) such that the time and space on catching and caching context window makes the practice inapplicable. The memory of attention matrices increases R^2 times as well, which further decelerates the throughput. Importantly, existing efficient attention mechanisms are not good at solving this dilemma because most of them focus

on decreasing the space and time expense of the attention computation instead of the linear mappings.

From the analysis of computation change, it can be known that the enlargement of the context window produces all of the extra computation costs. To address it simply, squeezing the patch covered by the large context window to the size of the local window can be an effective approach fully eliminating the large-window overhead, as shown in Fig. 1. b. But this way still needs substantial memory budgets to cache the large context patch, which means the inference speed becomes slow. Instead, we devise a strategy named densely overlapped mapping (DOM) layer, as shown in Fig. 1. c. The DOM layer is defined as a conv layer with a stride of 1, kernel sizes of (R, R) , in-out channel numbers of $(C, C/R^2)$, and the same padding mode, thereby outputting feature map $\in \mathbb{R}^{H \times W \times C/R^2}$. ‘Densely overlapped’ indicates the nearby kernels have large overlapping areas. The computation cost can be calculated by:

$$\Omega(\text{DOM}) = HW(R \times R)(C \times C/R^2) = HWC^2. \quad (3)$$

Clearly, DOM is computationally the same as the linear mapping layer, for which it is deemed as a mapping layer. The shape of large window is (RP, RP) , and the number of patches is $(\frac{H}{P} \times \frac{W}{P})$, so the memory used for context patches $\in \mathbb{R}^{(HW/P^2)(RP \times RP)C/R^2}$ is same as the query patches $\in \mathbb{R}^{(HW/P^2)(P \times P)C}$.

To align the shape of the context patch with the query patch, we use the sparsely overlapped mapping (SOM) layer to transform the output of DOM. The SOM layer is defined as a conv layer with strides of (R, R) , kernel sizes of (R, R) , and in-out channel numbers of $(C/R^2, C)$. For the context patches rearranged by the large context window sliding on the DOM’s output, the computation costs of SOM can be calculated by:

$$\begin{aligned} \Omega(\text{SOM}) &= HW/P^2 (P^2) (R \times R) (C/R^2 \times C) \\ &= HWC^2. \end{aligned} \quad (4)$$

Therefore, SOM acting on the context patches has the same computation cost as linear mapping layers on the input feature. The new context patches processed by SOM require no additional memory, with the same shape as query patches.

There is another potential risk associated with the large-window paradigm. The padding size of the large window is $\frac{(R-1)P}{2}$. In the edge area of a feature map, the context patch has a large portion of zeros. Such context patch makes the query patch just attend to a small area with valid representations, which makes the attention map meaningless as visualized in Fig. 1. d. To alleviate this issue, we propose a new padding mode that is equivalent to shifting the large window toward where the pixel is non-zero.

2.2. Lawin Transformer

The overall architecture is depicted in Fig. 1. e. In the CNN-dominant era, the last two stages of the backbone do not downsample the feature map so that the input size of the decoder is always one-eighth of the backbone’s input. Following this paradigm, Lawin Transformer firstly concatenates feature maps from the last three stages by resizing the last two feature maps (3rd and 4th stage) both to the same size as the 2nd-stage one, and then transform the concatenation with one linear layer to reduce the channel number. In the next step, Lawin attention will act on this output with the same size as the 2nd-stage feature map, which aims to obtain a trade-off between performance and efficiency.

The next step is the core of Lawin Transformer. To capture multi-scale representations, three Lawin attention mechanisms with different ratios R are paralleled. The size of the local window is determined dynamically, set to $(\frac{H}{8}, \frac{W}{8})$ that is subject to the size of the whole feature map. The ratios are set to 2, 4, and 8. Except for the three-scale representations, a short-cut branch and an image-pooling module are added to consummate multi-scale representations, motivated by [1]. The MLP of Lawin Transformer consists of two layers. The first layer is a linear layer performing channel reduction for feature aggregation.

The second layer of MLP empowers the output of the first layer with low-level representations. As aforementioned, the 1st-stage feature is the most spatially informative

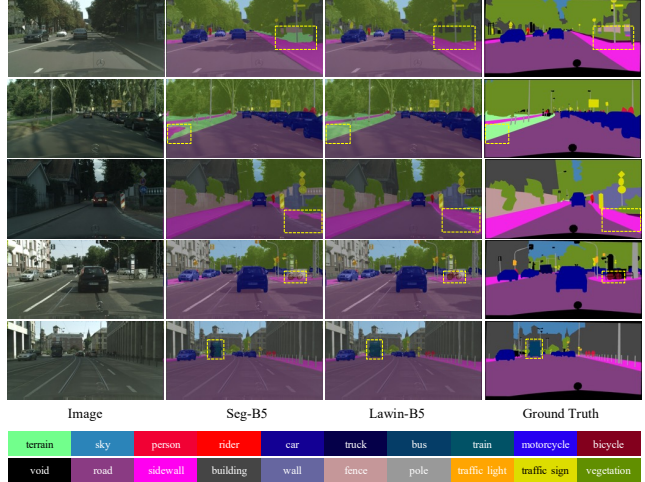


Figure 2. Visualization Comparison of Lawin Transformer with SegFormer on Cityscapes.

but performing computation on it takes the most costs. In terms of the balance between performance and efficiency, before leveraging it a lightweight linear layer reduces its channel numbers. Besides, the output of the first layer is interpolated to the same size as the 1st-stage feature (by up-sampling ratio 2) and concatenated with it. Then the second layer of MLP fuses the concatenation for the final per-pixel classifier or mask classifier [3].

3. Experiment

3.1. Dataset and Implementation

We conduct experiments on two public datasets including Cityscapes [4] and ADE20K [12]. Our hardware environment is a server with 4 NVIDIA GTX3090 GPUs. All of the other methods’ results reported in this section are obtained by our training official repos.

3.2. Comparison with SegFormer

The MLP-decoder designed by SegFormer is a simple and effective way to leverage multi-level features from the backbone. To reveal the superiority of Lawin Transformer, table 1 shows the comparison of parameters, FLOPs, and mIoU. Across all variants of MiT (B0→B5), our combination trumps SegFormer on every metric. Moreover, segmentation masks are visualized to qualitatively show superiority. As depicted in Fig. 2, the yellow dotted box covers the noteworthy region. In the second row, some small areas of the terrain are left unlabeled by SegFormer due to the occlusion of shadow, but Lawin distinguishes them consistently. In the last row, SegFormer wrongly labels pixels of the train as cars or trucks, and Lawin labels these correctly.

3.3. Comparison with ConvNext-UpperNet

UpperNet is the most widely used semantic segmentation decoder for new-era backbones. We choose ConvNext as

Dataset	ADE20K			Cityscapes
Method	Params ↓	FLOPs↓	SS/MS↑	SS/MS↑
Seg-B0	3.8	8.4	38.1 / 38.6	76.5 / 78.2
Lawin-B0	3.3	5.3	38.9 / 39.6	77.2 / 78.7
Seg-B1	13.7	15.9	41.7 / 42.8	78.5 / 80.0
Lawin-B1	13.4	12.7	42.1 / 43.1	79.0 / 80.4
Seg-B2	27.5	62.4	46.5 / 47.5	81.0 / 82.2
Lawin-B2	24.2	45.0	47.8 / 48.8	81.7 / 82.7
Seg-B3	47.3	79.0	48.7 / 49.2	81.7 / 83.3
Lawin-B3	44.0	61.7	50.3 / 51.1	82.5 / 83.7
Seg-B4	64.1	95.7	49.6 / 50.4	82.2 / 83.6
Lawin-B4	61.8	78.2	50.7 / 51.4	82.7 / 84.0
Seg-B5	84.7	183.3	50.7 / 51.2	82.3 / 83.7
Lawin-B5	84.1	159.1	52.3 / 53.0	82.8 / 84.3

Table 1. Comparison of SegFormer with Lawin Transformer.

Dataset	ADE20K			Cityscapes
Method	Params ↓	FLOPs↓	SS/MS↑	SS/MS↑
Uper-T	60.2	234.7	46.1 / 46.7	80.2 / 80.8
Lawin-T	34.7	52.6	47.4 / 48.1	80.7 / 81.4
Uper-S	81.9	256.8	48.5 / 49.1	81.5 / 82.3
Lawin-S	56.3	74.7	48.8 / 49.9	82.0 / 82.8
Uper-B	122.1	292.4	52.3 / 52.7	82.4 / 83.2
Lawin-B	94.6	109.8	53.3 / 54.2	82.8 / 83.8
Uper-L	235.0	393.3	53.1 / 53.4	83.1 / 83.6
Lawin-L	203.8	209.7	54.2 / 55.0	83.1 / 83.9
Uper-XL	391.1	533.6	53.6 / 54.2	83.2 / 83.9
Lawin-XL	356.1	348.9	54.5 / 55.3	83.5 / 84.4

Table 2. Comparison of ConvNext-UperNet with Lawin Transformer.

the backbone to compare Lawin Transformer with UperNet, as shown in table 2. The ConvNext-Lawin combination consistently uses fewer FLOPs and parameters to achieve performance gains on each capacity backbone.

3.4. Comparison with Swin-FPN-MaskFormer

MaskFormer [3] utilizes FPN to aggregate the multi-level feature maps. Table 3 showcases Lawin outperforms FPN by large margins at almost identical computation costs.

3.5. Ablation Study

Context Aggregation Module. The parallel branch architecture of Lawin attention described in sec. 2.2 can be deemed as an plug-n-play part. We are interested in the consequence of replacing it with popular multi-scale context aggregation modules in the CNN-dominant era, such as pyramid pooling module (PPM) [11], atrous spatial pyramid pooling (ASPP) [1], and separable ASPP (SEP-ASPP) [2]. Table 4 reports FLOPs, parameters, and mIoU of these classical methods along with ours. PPM and SEP-ASPP are more computationally efficient than Lawin, but the performance gap is substantial. It is evident that Lawin attention is at the sweet point between performance and efficiency as a new-era context aggregation module.

Method	MLA	Params ↓	FLOPs↓	SS/MS↑
SwinMask-T	FPN	41.8	57.3	46.6 / 48.5
	Lawin	43.2	55.8	47.4 / 49.2
SwinMask-S	FPN	63.1	81.1	49.5 / 50.6
	Lawin	64.5	80.3	50.5 / 52.7
SwinMask-B	FPN	102	198.3	52.5 / 53.7
	Lawin	101.4	198	53.7 / 54.5
SwinMask-L	FPN	212	378	54.0 / 55.3
	Lawin	211.5	377	55.3 / 56.5

Table 3. Comparison of FPN with Lawin Transformer when serving as the MLA module.

Method	FLOPs(G)↓	Params(M) ↓	SS/MS↑
PSP [11]	48.2	49.8	47.8 / 48.7
ASPP [1]	82.9	57.0	48.7 / 49.5
SEP-ASPP [2]	57.2	50.7	48.4 / 49.3
Lawin attention	61.7	49.5	49.9 / 50.9

Table 4. Results of different context aggregation modules when coupled with MiT-B3 on ADE20K.

Low	Short	R=2	R=4	R=8	Pool	Padding	SS
✓	✓	✗	✓	✓	✓	✓	49.3
✓	✓	✓	✗	✓	✓	✓	49.4
✓	✓	✓	✓	✗	✓	✓	49.4
✓	✗	✓	✓	✓	✓	✓	49.6
✓	✓	✓	✓	✓	✗	✓	49.3
✗	✓	✓	✓	✓	✓	✓	49.1
✓	✓	✓	✓	✓	✓	✗	49.2
✓	✓	✓	✓	✓	✓	✓	49.9

Table 5. Results of Lawin-B3 on ADE20k when different branches are absent.

Scale and Padding. Our method captures multi-scale representations through Lawin attention, short-cut branch, image-pooling module, and low-level representations. Table 5 studies the impact of removing any scale (from Low to Pool). For Lawin ones, the performance drops 0.6%, 0.5%, and 0.5% due to removing the branch with ratio 2, 4, or 8, respectively. We also verify the effectiveness of Lawin padding mode by manifesting that zero padding can yield a performance drop of 0.7%.

4. Conclusion

This paper introduces Lawin Transformer, an MLA module tailored to new-era backbones. Empirical results demonstrate that Lawin Transformer exhibits outstanding performance to serve as a new-era semantic segmentation decoder, owing to its computational efficiency and simplicity. The core of Lawin Transformer, the parallel architecture of Lawin attention, proves to be a powerful module for aggregating contextual information at multiple scales. We envision Lawin Transformer as a substitute for UperNet in future research on vision backbones. Furthermore, we anticipate that Lawin attention can find applications in capturing multi-scale representations across various fields.

References

- [1] Liang-Chieh Chen, George Papandreou, Florian Schroff, and Hartwig Adam. Rethinking atrous convolution for semantic image segmentation. *arXiv*, 2017. 3, 4
- [2] Liang-Chieh Chen, Yukun Zhu, George Papandreou, Florian Schroff, and Hartwig Adam. Encoder-decoder with atrous separable convolution for semantic image segmentation. In *ECCV*, 2018. 4
- [3] Bowen Cheng, Alexander G. Schwing, and Alexander Kirillov. Per-pixel classification is not all you need for semantic segmentation. In *NeurIPS*, 2021. 1, 3, 4
- [4] Marius Cordts, Mohamed Omran, Sebastian Ramos, Timo Rehfeld, Markus Enzweiler, Rodrigo Benenson, Uwe Franke, Stefan Roth, and Bernt Schiele. The cityscapes dataset for semantic urban scene understanding. In *CVPR*, 2016. 3
- [5] Alexey Dosovitskiy, Lucas Beyer, Alexander Kolesnikov, Dirk Weissenborn, Xiaohua Zhai, Thomas Unterthiner, Mostafa Dehghani, Matthias Minderer, Georg Heigold, Sylvain Gelly, et al. An image is worth 16x16 words: Transformers for image recognition at scale. In *ICLR*, 2020. 1
- [6] Meng-Hao Guo, Cheng-Ze Lu, Qibin Hou, Zhengning Liu, Ming-Ming Cheng, and Shi-Min Hu. Segnext: Rethinking convolutional attention design for semantic segmentation. *arXiv preprint arXiv:2209.08575*, 2022. 1
- [7] Ze Liu, Yutong Lin, Yue Cao, Han Hu, Yixuan Wei, Zheng Zhang, Stephen Lin, and Baining Guo. Swin transformer: Hierarchical vision transformer using shifted windows. In *ICCV*, 2021. 1
- [8] Zhuang Liu, Hanzi Mao, Chao-Yuan Wu, Christoph Feichtenhofer, Trevor Darrell, and Saining Xie. A convnet for the 2020s. *Proceedings of the IEEE/CVF Conference on Computer Vision and Pattern Recognition (CVPR)*, 2022. 1
- [9] Tete Xiao, Yingcheng Liu, Bolei Zhou, Yuning Jiang, and Jian Sun. Unified perceptual parsing for scene understanding. In *ECCV*, 2018. 1
- [10] Enze Xie, Wenhai Wang, Zhiding Yu, Anima Anandkumar, Jose M Alvarez, and Ping Luo. Segformer: Simple and efficient design for semantic segmentation with transformers. In *NeurIPS*, 2021. 1
- [11] Hengshuang Zhao, Jianping Shi, Xiaojuan Qi, Xiaogang Wang, and Jiaya Jia. Pyramid scene parsing network. In *CVPR*, 2017. 4
- [12] Bolei Zhou, Hang Zhao, Xavier Puig, Sanja Fidler, Adela Barriuso, and Antonio Torralba. Scene parsing through ade20k dataset. In *CVPR*, 2017. 3